Diurnal temperature range expands with warming for temperatures above the melting point

Felix Pithan[1], **Leonhard Schatt**[1,2]

[1]Alfred Wegener Institute, Helmholtz Centre for Polar and Marine Research, Bremerhaven, Germany
[2]University of Bayreuth, Bayreuth, Germany

Key Points:

- The diurnal temperature range (DTR) has a local minimum near 0°C.
- DTR in observations shrinks strongly for temperatures below 0°C and expands for warmer temperatures.
- Climate models that reproduce the local DTR minimum near 0°C show a significant slowdown of DTR shrinking in recent decades.

Corresponding author: Felix Pithan, `felix.pithan@awi.de`

Abstract

The globally averaged diurnal temperature range (DTR) has shrunk since the mid-20th century, and climate models project further shrinking. Observations indicate a slowdown or reversal of this trend in recent decades. Here, we show that DTR has a minimum for average temperatures close to 0°C. Observed DTR shrinks strongly at colder temperature, where warming shifts the average temperature towards the DTR minimum, and expands at warmer temperature, where warming shifts the average temperature away from the DTR minimum. Most, but not all climate models reproduce the minimum DTR close to 0°C and a stronger DTR shrinking at colder temperature. In models that reproduce the DTR minimum close to 0°C, DTR shrinking slows down significantly in recent decades. Model projections suggest that the DTR will resume or continue shrinking over the 21st century.

Plain Language Summary

The diurnal temperature range, i.e. the average difference between daily maximum and minimum temperatures, affects both human health and plant development. Global datasets have shown a shrinking diurnal temperature range since the 1950s, but a recent study found that the diurnal temperature range had increased again. In this study, we investigate how the diurnal temperature range behaves at different mean temperatures. We find that the diurnal temperature range is particularly small for temperatures close to the melting point of water (0°C), and larger for both colder and warmer temperatures. This is caused by the latent heat of freezing/melting, which makes it much harder to warm the soil from -1°C to +1°C than from -3°C to -1°C or from 1°C to 3°C. The diurnal temperature range shrinks in regions and seasons with negative average temperature, where global warming pushes the average closer to 0°C and expands for warmer temperature. Most, but not all climate models also show a narrow diurnal temperature range near 0°C, shrinking of the temperature range at colder temperature and a slower reduction in the diurnal temperature range in recent decades. Models suggest that the currently observed growth of the diurnal temperature range is a transient phenomenon.

1 Introduction

The diurnal temperature range (DTR), or difference between daily minimum and maximum temperature, is an important climate indicator (Braganza et al., 2004) with substantial effects on human health (Cheng et al., 2014) and crop yields (Lobell, 2007). The global-mean diurnal temperature range over land areas has decreased over the second half of the 20th century, in particular between 1960 and 1980 (Gulev et al., 2021). Some areas, mostly in the midlatitudes, have experienced positive DTR trends. Huang et al. (2023) recently reported that the global trend had reversed, and DTR over global land areas had increased between 1980 and 2021.

Changes in the diurnal temperature range have been attributed to changes in cloud cover (Dai et al., 1997, 1999; Doan et al., 2022), with increases in cloud cover dampening both daytime warming from incoming solar radiation and nighttime longwave radiative cooling. Observed decreases ('solar dimming' until about 1980) and increases ('solar brightening' since about 1980 over Europe and 2005 over China) of incoming solar radiation at the surface (Schwarz et al., 2020), partly due to changes in air pollution, particularly affect daily maximum temperature and thus DTR. Land-surface feedbacks such as increased heating of dry soils during droughts and heatwaves further affect maximum temperatures and the diurnal temperature range (Zhou et al., 2009; Daramola et al., 2024), whereas temperature feedbacks in the stable boundary layer particularly affect nighttime temperatures (Walters et al., 2007).

Lindvall and Svensson (2015) found that climate models of the 5th coupled model intercomparison project (CMIP5) mostly underestimated the diurnal temperature range compared to observations. Most models agreed on an overall decrease in DTR over the historical period and in future projections with continued increases in greenhouse gas concentrations. CMIP6 models also tend to underestimate DTR and project further decreases for the 21st century, except under the low-emission scenario SSP1-2.6 (Wang et al., 2024).

In this paper, we focus on the role of the melting/freezing point for the diurnal temperature range and DTR trend in a changing climate. Stone and Weaver (2003) noted that in the CCCma climate models, mid-latitude DTR had a minimum close to mean temperatures of 0°C, but to our knowledge this has not yet been investigated in observations or linked to the spatial, temporal and seasonal variations in DTR trends.

2 Data

2.1 Station observations

We use station observations of the surface air temperature measured 2m above the ground from the Neumayer research station (Wesche et al., 2016) in Antarctica (1983-2022) and the AWIPEV research base in Ny Ålesund, Svalbard (1994-2022). The Neumayer station is situated on the Ekström Ice shelf at 70.7 °S, 8.3 °W, and the AWIPEV research based in the Kongsfjord at 78.9 °N, 11.9°E. Both stations are close to the ocean, which is covered with sea ice during most of the year close to Neumayer. Kongsfjorden close to Ny Ålesund has usually remained ice-free throughout the winter in the last decade. We derive the diurnal temperature range and daily average temperature from the original data provided with a frequency of 10 minutes.

2.2 Gridded temperature data

We use average temperature and the diurnal temperature range from the CRU land temperature dataset CRU TS v4 (Harris et al., 2020), a quality-controlled homogenized dataset of monthly gridded data based on global station observations (Harris et al., 2014) of surface air temperature. We restrict our evaluation to grid points that include at least one station for interpolation throughout the entire timeframe considered.

2.3 CMIP6 model output

We use monthly means of daily maximum, daily minimum and average temperature (tasmax,tasmin,tas) for 1950-2014 from the historical runs of the 6th coupled model intercomparison project (CMIP6, Eyring et al. (2016)). Each model's land-sea mask (sftlf) is used to select grid points with at least 90 % land coverage. We analysed all models for which the required data was available at the DKRZ ESGF node (see Table 1).

3 Results and discussion

3.1 Temperature-dependance and seasonal cycle of DTR

Binning the diurnal temperature range observed at AWIPEV and the Neumayer station according to the daily average temperature (Figure 1) shows that the DTR decreases with increasing average temperature between about -10 °C and 0 °C. This effect it surprisingly consistent between the two stations. Especially the smallest DTR are lower at Neumayer than AWIPEV, likely due to the much more homogeneous terrain and full year-round snowcover at Neumayer.

Table 1. Models used in the analysis. AWI-CM-1-1-MR was excluded from the plots as an outlier.

model	CMIP data doi
ACCESS-CM2	10.22033/ESGF/CMIP6.4271
ACCESS-ESM1-5	10.22033/ESGF/CMIP6.4272
AWI-CM-1-1-MR	
AWI-ESM-1-1-LR	10.22033/ESGF/CMIP6.9328
CMCC-ESM2	10.22033/ESGF/CMIP6.13195
CanESM5	10.22033/ESGF/CMIP6.3610
EC-Earth3	10.22033/ESGF/CMIP6.4700
EC-Earth3-AerChem	10.22033/ESGF/CMIP6.4701
EC-Earth3-Veg	10.22033/ESGF/CMIP6.727
EC-Earth3-Veg-LR	10.22033/ESGF/CMIP6.4707
FGOALS-g3	10.22033/ESGF/CMIP6.3356
GFDL-ESM4	10.22033/ESGF/CMIP6.8597
INM-CM4-8	10.22033/ESGF/CMIP6.5069
INM-CM5-0	10.22033/ESGF/CMIP6.5070
IPSL-CM6A-LR	10.22033/ESGF/CMIP6.5195
MIROC6	10.22033/ESGF/CMIP6.5603
MPI-ESM-1-2-HAM	10.22033/ESGF/CMIP6.5016
MPI-ESM1-2-HR	10.22033/ESGF/CMIP6.6594
MPI-ESM1-2-LR	10.22033/ESGF/CMIP6.6595
MRI-ESM2-0	10.22033/ESGF/CMIP6.6842
SAM0-UNICON	10.22033/ESGF/CMIP6.7789

We attribute the effect of the freezing/melting point on DTR to the increased latency of surface temperature close to the phase change of water: When the surface is frozen, it cannot easily warm beyond 0 °C without first melting the frozen ground moisture or snowpack. When no snow is present, ground moisture needs to freeze, releasing latent heat, before the ground can cool below 0 °C. These constraints are not effective on days with an average temperature below -10 °C or above 10 °C, as the typical range of diurnal temperature variability for such days does not encompass 0 °C. This effect of mean temperatures on the DTR near 0 °C has been reported by Stone and Weaver (2003) for CCCma climate model output, but not previously been shown in observations or evaluated in climate models.

Correlations between the DTR and relative humidity, sunshine duration, surface pressure and near-surface wind speeds in Ny Ålesund observations are substantially lower than those between DTR and average temperature both on daily (not shown) and monthly time scales (Figure S1).

Plotting each month's DTR against its mean temperature for the high-latitude land areas represented in the CRU dataset (Figure 2) supports the existence of a DTR minimum close to 0°C. The DTR has a seasonal cycle that goes beyond the temperature-dependence, with spring showing a higher DTR than autumn for a similar average temperature. From September through February, mean temperature decreases and the DTR expands accordingly, but from February to April, the DTR continues to expand to its highest values while the average temperature also increases. The DTR then shrinks again with further increasing temperature until the mean temperature reaches 0°C in June, and DTR expands with mean temperature warming beyond 0°C in July and August. We attribute this seasonal cycle to the presence of snow and a higher solar zenith angle during spring than autumn for comparable mean temperatures (Cerveny & Balling Jr, 1992). Snow has a low heat capacity and conductivity, which leads to a low effective heat ca-

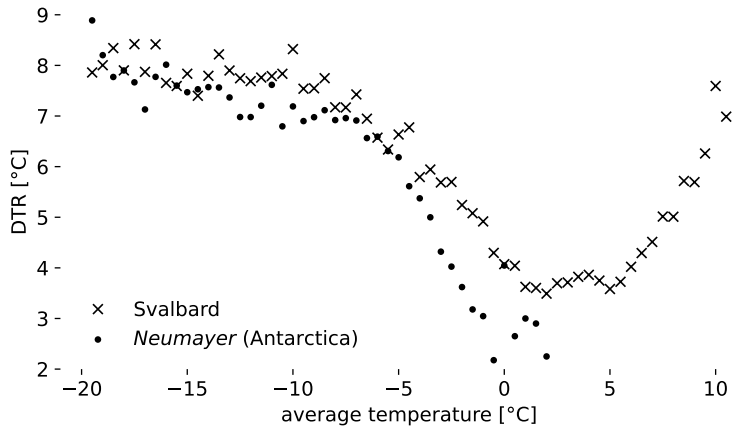

Figure 1. Diurnal temperature range observed at AWIPEV (1994-2022) and Neumayer (1983-2022), binned according to average temperatures.

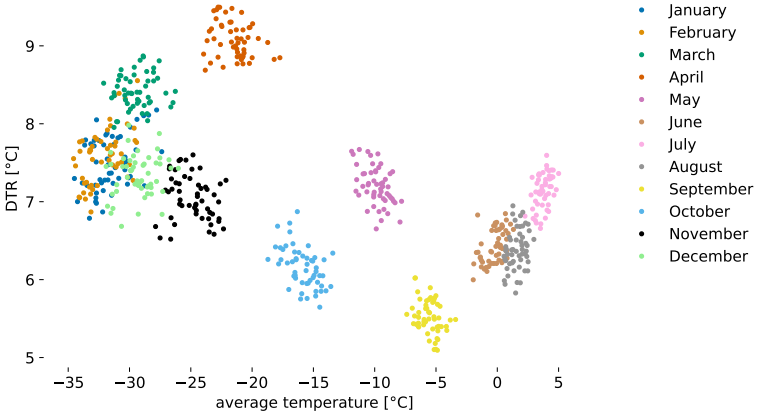

Figure 2. Diurnal temperature range for CRU data, binned according to average temperatures. Each point represents data from an individual month in the period 1970-2022 averaged over the land area between 70 ° N and 90 ° N.

pacity at the surface and thus a strong response of the surface temperature to imbalances in the surface energy budget, which contribute to a larger DTR. Higher maxima of solar radiation contribute to a larger diurnal cycle in the surface energy budget and thereby to a larger DTR.

3.2 Seasonality and temperature-dependence of DTR trends

DTR is mostly shrinking in months and places with an average temperature below 0°C, and expanding at warmer average temperature (Figure 3) This holds across seasons with some variance in the temperature threshold for positive/negative trends (Figure 3 a). Binning trends according to average temperature (Figure 3 b) shows the strongest DTR shrinking below an average temperature of -10°C. Negative DTR trends for temperatures below the 0 °C and positive DTR trends for positive temperatures are consistent with the temperature-dependence of DTR shown above.

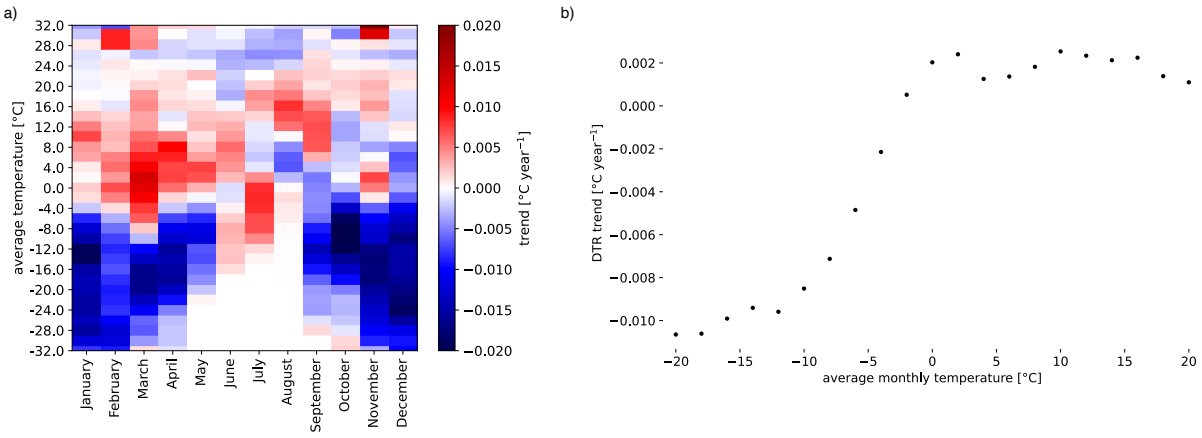

Figure 3. a) DTR trends in the CRU dataset (1970-2022) as a function of calendar month and mean temperaure, b) DTR trends binned as a function of monthly mean temperature.

In addition to the melting point effect on DTR, the maximum temperature during dry, hot summers, increases more strongly than the average and minimum temperature because dry soils are no longer cooled by evaporation. This additional increase in maximum temperatures leads to an increase in DTR in areas affected by droughts (Daramola et al., 2024).

3.3 Temperature-dependence of DTR and its trend in CMIP6 models

Most CMIP6 models reproduce the observed relationship between DTR and mean temperature with a minimum DTR near the melting point (Figure 4). A notable exception are the different variants of the EC-Earth model, which only show a stagnation of the increase in DTR with temperature near 0°C, but no local minimum. In the other models, the difference between the DTR minimum and the DTR at lower and higher temperatures ranges from about 1°C to about 6°C. For further analyses, we distinguish models with no or a weak melting-point effect and thus DTR minimum near 0°C, marked by dashed lines in (Figure 4), from models with a local DTR minimum more than 1°C below the highest DTR at colder temperature. Observations point towards a substantially larger effect, so our assessment of differences between these groups of models is a conservative estimate.

The DTR itself also has a strong inter-model spread, ranging from 4 to 10°C for an average temperature around 0°C when excluding the outlier model AWI-CM-1-1-MR with a DTR around 20°C. While a full evaluation of the DTR in climate models is beyond the scope of this paper, our high-latitude observations indicate typical DTR around 8°C for average temperatures below -10°C. This would be on the upper end of the CMIP6 inter-model spread at similar average temperature, consistent with earlier findings that CMIP5 climate models tend to underestimate DTR (Lindvall & Svensson, 2015).

For surface air temperatures above the local minimum near 0°C, climate models agree on a general expansion of DTR with increasing temperature, with a second local minimum near 25°C. This might seem at odds with a general trend of shrinking DTR with global warming, but the effect of anthropogenic climate change on DTR partly occurs as a rapid adjustment, i.e. a direct response to the increased greenhouse gas concentration and its radiative effects that is independent of surface temperature change (Jackson & Forster, 2013). The response of DTR to climate change thus cannot be expected to follow the temperature-DTR relationship in a given climate state.

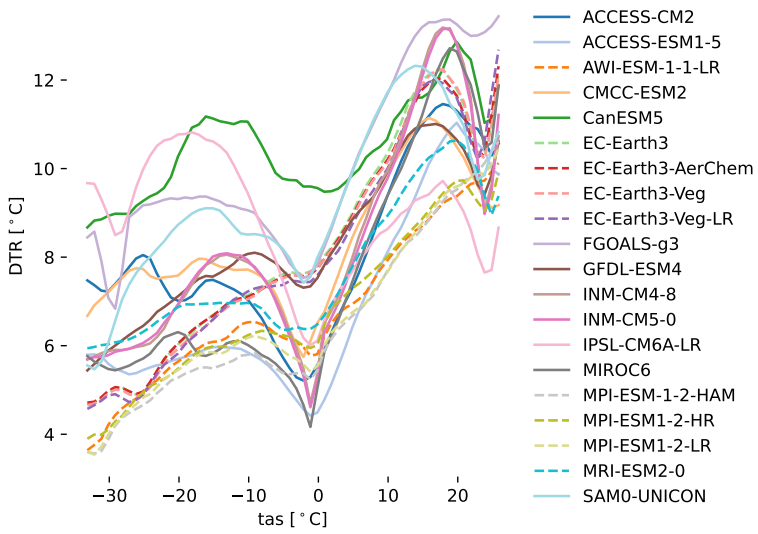

Figure 4. Diurnal temperature range as a function of monthly mean surface air temperature (tas) in CMIP6 climate models (historical run, 1950-2014). Dashed lines show models with a particularly weak representation of melting-point effect on DTR.

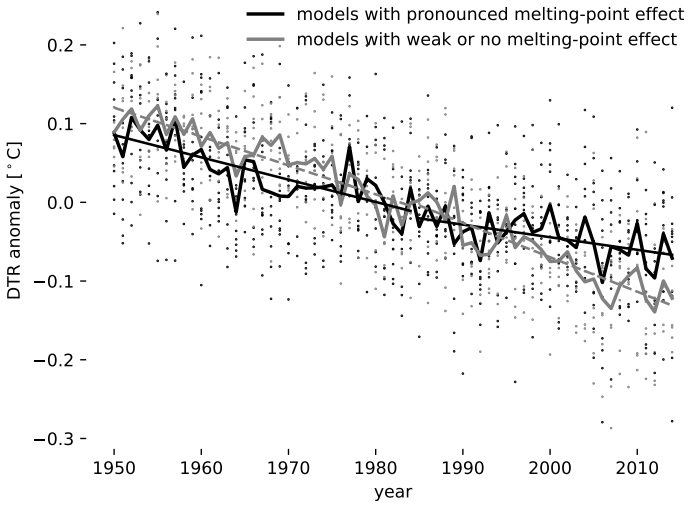

Figure 5. Annual mean diurnal temperature range in CMIP6 climate models (historical run) over global land areas and linear trends before and after 1985. Dots represent individual models, and lines the mean over models with a substantial DTR minimum near 0°C (black) or a weak or no DTR minimum (gray, corresponding to models shown with dahed lines in Figure 4)

Computing global DTR trends for models with no or a weak representation of the melting-point effect on DTR separately from models with a substantial melting-point effect (Figure 5) shows that the latter display a significantly (p=0.02 for a one-sided Welch t-test) weaker DTR shrinking after than prior to 1985. In models with a weak or no melting-point effect, the DTR continues shrinking with no significant difference between the earlier and later period.

Model reproduce substantial shrinking of the DTR at average temperature below 0°C, and weaker shrinking or expansion of the DTR for temperatures around 10 °C (Figure S1). The 1970-2014 inter-model average shows an expansion of the DTR for an average temperature around 10 °C when excluding models with a weak or no DTR minimum at 0°C.

4 Conclusions

The DTR strongly depends on average temperatures in the (average) temperature range from -10 °C to 10 °C, with a minimum DTR near 0 °C and larger DTR for both warmer and colder temperatures. Beyond this temperature range, climate models indicate mostly larger DTR with larger average temperatures and a second minimum above 25 °C.

This relationship is not the major driver for shrinking DTR in response to global warming (Jackson & Forster, 2013), but it affects global DTR trends on decadal to multidecadal time scales and their seasonal and geographical distribution. Observed DTR trends in recent decades are predominantly shrinking below 0°C and expanding above 0°C, consistent with the melting-point effect on DTR. In addition to the melting-point effect, land-surface feedbacks due to drying and reduced evaporation in summer contribute to positive trends at warmer temperature (Daramola et al., 2024).

Climate models that represent the minimum DTR near 0 °C show a weaker shrinking of global-mean DTR in recent decades, whereas models that (largely) lack this minimum simulate a steadily shrinking DTR. The DTR trend in models that represent the melting-point effect on DTR is thus more consistent with observations suggesting a recent growth in DTR (Huang et al., 2023).

The lack of a DTR minimum near 0 °C in some models points to issues in atmosphere-surface coupling that should be further investigated. The substantial inter-model spread in DTR (on the order of 5 °C for a given average temperature) could also be leveraged to evaluate atmosphere-surface coupling in models. We further suggest to investigate the mechanisms behind the second minimum in DTR above 25 °C and compare this feature in models to observations from lower latitudes.

Open Research Section

Temperature data and other meteorological observations from Neumayer (Schmithüsen, 2023) and Ny-Alesund (Maturilli, 2020) are provided by the Alfred Wegener institute and available from the PANGAEA database (https://doi.org/10.1594/PANGAEA.962313, https://doi.org/10.1594/PANGAEA.914979). The CRU temperature dataset (Harris et al., 2020) is provided by the Climatic Research Unit (University of East Anglia) and NCAS.

Acknowledgments

We thank station staff at AWIPEV and Neumayer for carrying out the long-term observations used in the paper, the Climate Research Unit for providing its temperature dataset and the climate modelling groups participating in CMIP6 for making available their model output. Thanks to Christof Luepkes for comments on an earlier version of

this manuscript, and to Marion Maturilli and Holger Schmidthüsen for support in accessing and using the station observations. This work has partly been funded by the European Union (ERC, A3m-transform, 101076205). Views and opinions expressed are however those of the authors only and do not necessarily reflect those of the European Union or the European Research Council Executive Agency. Neither the European Union nor the granting authority can be held responsible for them. LS acknowledges support by the Elite Network of Bavaria (ENB) through the study program "Macromolecular Science".

References

Braganza, K., Karoly, D. J., & Arblaster, J. M. (2004). Diurnal temperature range as an index of global climate change during the twentieth century. *Geophysical research letters*, *31*(13).

Cerveny, R. S., & Balling Jr, R. C. (1992). The impact of snow cover on diurnal temperature range. *Geophysical research letters*, *19*(8), 797–800.

Cheng, J., Xu, Z., Zhu, R., Wang, X., Jin, L., Song, J., & Su, H. (2014). Impact of diurnal temperature range on human health: a systematic review. *International journal of biometeorology*, *58*, 2011–2024.

Dai, A., Genio, A. D. D., & Fung, I. Y. (1997). Clouds, precipitation and temperature range. *Nature*, *386*(6626), 665–666.

Dai, A., Trenberth, K. E., & Karl, T. R. (1999). Effects of clouds, soil moisture, precipitation, and water vapor on diurnal temperature range. *Journal of Climate*, *12*(8), 2451–2473.

Daramola, M. T., Li, R., & Xu, M. (2024). Increased diurnal temperature range in global drylands in more recent decades. *International Journal of Climatology*, *44*(2), 521–533.

Doan, Q.-V., Chen, F., Asano, Y., Gu, Y., Nishi, A., Kusaka, H., & Niyogi, D. (2022). Causes for asymmetric warming of sub-diurnal temperature responding to global warming. *Geophysical Research Letters*, *49*(20), e2022GL100029.

Eyring, V., Bony, S., Meehl, G. A., Senior, C. A., Stevens, B., Stouffer, R. J., & Taylor, K. E. (2016). Overview of the coupled model intercomparison project phase 6 (cmip6) experimental design and organization. *Geoscientific Model Development*, *9*(5), 1937–1958.

Gulev, S., Thorne, P., Ahn, J., Dentener, F., Domingues, C., Gerland, S., ... Vose, R. (2021). Changing state of the climate system [Book Section]. In V. Masson-Delmotte et al. (Eds.), *Climate change 2021: The physical science basis. contribution of working group i to the sixth assessment report of the intergovernmental panel on climate change* (pp. 287–422). Cambridge, United Kingdom and New York, NY, USA: Cambridge University Press. doi: 10.1017/9781009157896.004

Harris, I., Jones, P. D., Osborn, T. J., & Lister, D. H. (2014). Updated high-resolution grids of monthly climatic observations–the cru ts3. 10 dataset. *International journal of climatology*, *34*(3), 623–642.

Harris, I., Osborn, T. J., Jones, P., & Lister, D. (2020). Version 4 of the cru ts monthly high-resolution gridded multivariate climate dataset. *Scientific Data*, *7*, 109. Retrieved from `https://doi.org/10.1038/s41597-020-0453-3` doi: 10.1038/s41597-020-0453-3

Huang, X., Dunn, R. J., Li, L. Z., McVicar, T. R., Azorin-Molina, C., & Zeng, Z. (2023). Increasing global terrestrial diurnal temperature range for 1980–2021. *Geophysical Research Letters*, *50*(11), e2023GL103503.

Jackson, L. S., & Forster, P. M. (2013). Modeled rapid adjustments in diurnal temperature range response to co2 and solar forcings. *Journal of Geophysical Research: Atmospheres*, *118*(5), 2229–2240.

Lindvall, J., & Svensson, G. (2015). The diurnal temperature range in the cmip5 models. *Climate Dynamics*, *44*, 405–421.

Lobell, D. B. (2007). Changes in diurnal temperature range and national cereal yields. *Agricultural and forest meteorology*, *145*(3-4), 229–238.

Maturilli, M. (2020). *Continuous meteorological observations at station ny-ålesund (2011-08 et seq).* Alfred Wegener Institute - Research Unit Potsdam, PANGAEA. PANGAEA. Retrieved from `https://doi.org/10.1594/PANGAEA.914979` doi: 10.1594/PANGAEA.914979

Schmithüsen, H. (2023). *Continuous meteorological observations at neumayer station (1982-03 et seq).* Alfred Wegener Institute, Helmholtz Centre for Polar and Marine Research, Bremerhaven, PANGAEA. PANGAEA. Retrieved from `https://doi.org/10.1594/PANGAEA.962313` doi: 10.1594/PANGAEA.962313

Schwarz, M., Folini, D., Yang, S., Allan, R. P., & Wild, M. (2020). Changes in atmospheric shortwave absorption as important driver of dimming and brightening. *Nature Geoscience*, *13*(2), 110–115.

Stone, D., & Weaver, A. (2003). Factors contributing to diurnal temperature range trends in twentieth and twenty-first century simulations of the cccma coupled model. *Climate Dynamics*, *20*(5), 435–445.

Walters, J. T., McNider, R. T., Shi, X., Norris, W. B., & Christy, J. R. (2007). Positive surface temperature feedback in the stable nocturnal boundary layer. *Geophysical Research Letters*, *34*(12).

Wang, S., Zhang, M., Tang, J., Yan, X., Fu, C., & Wang, S. (2024). Interannual variability of diurnal temperature range in cmip6 projections and the connection with large-scale circulation. *Climate Dynamics*, 1–16.

Wesche, C., Weller, R., König-Langlo, G., Fromm, T., Eckstaller, A., Nixdorf, U., & Kohlberg, E. (2016). Neumayer iii and kohnen station in antarctica operated by the alfred wegener institute. *Journal of large-scale research facilities JLSRF*, *2*, A85–A85.

Zhou, L., Dai, A., Dai, Y., Vose, R. S., Zou, C.-Z., Tian, Y., & Chen, H. (2009). Spatial dependence of diurnal temperature range trends on precipitation from 1950 to 2004. *Climate Dynamics*, *32*, 429–440.

Figure 3.

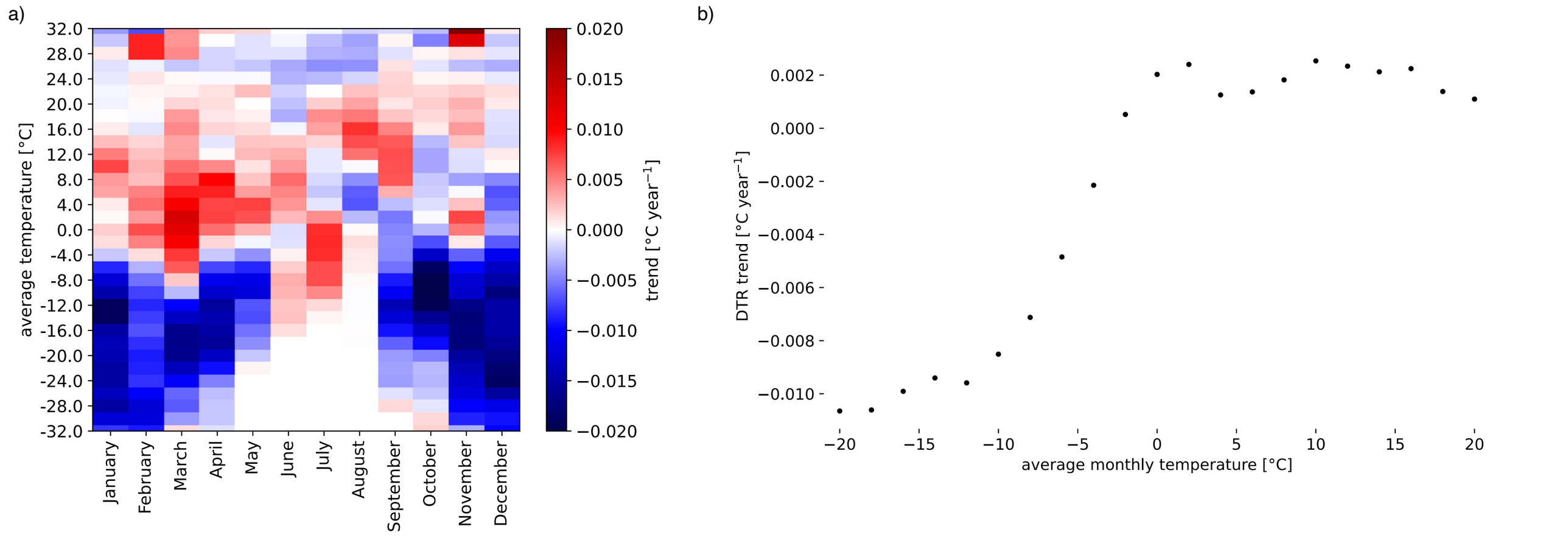
a)
32.0
28.0
24.0
20.0
16.0
12.0
8.0
4.0
0.0
-4.0
-8.0
-12.0
-16.0
-20.0
-24.0
-28.0
-32.0
average temperature [°C]
January
February
March
April
May
June
July
August
September
October
November
December
0.020
0.015
0.010
0.005
0.000
−0.005
−0.010
−0.015
−0.020
trend [°C year^{-1}]
b)
0.002
0.000
−0.002
−0.004
−0.006
−0.008
−0.010
DTR trend [°C year^{-1}]
−20
−15
−10
−5
0
5
10
15
20
average monthly temperature [°C]

Figure 5.

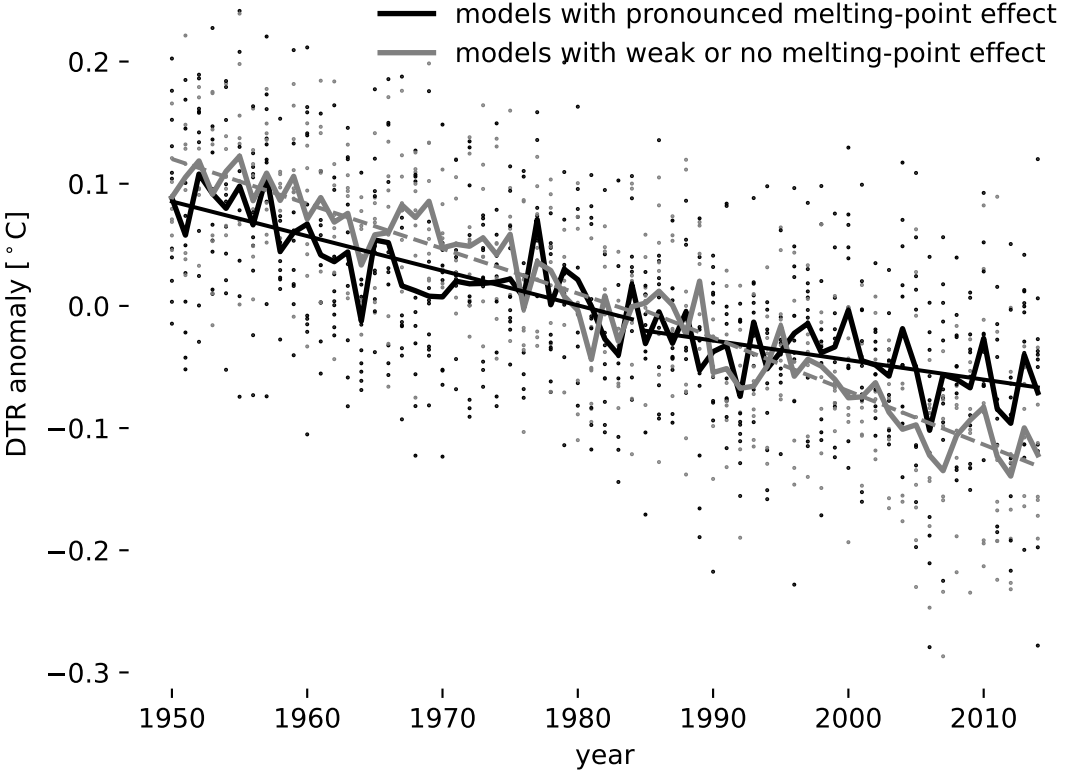
models with pronounced melting-point effect
models with weak or no melting-point effect
DTR anomaly [° C]
0.2
0.1
0.0
−0.1
−0.2
−0.3
1950
1960
1970
1980
1990
2000
2010
year

Figure 4.

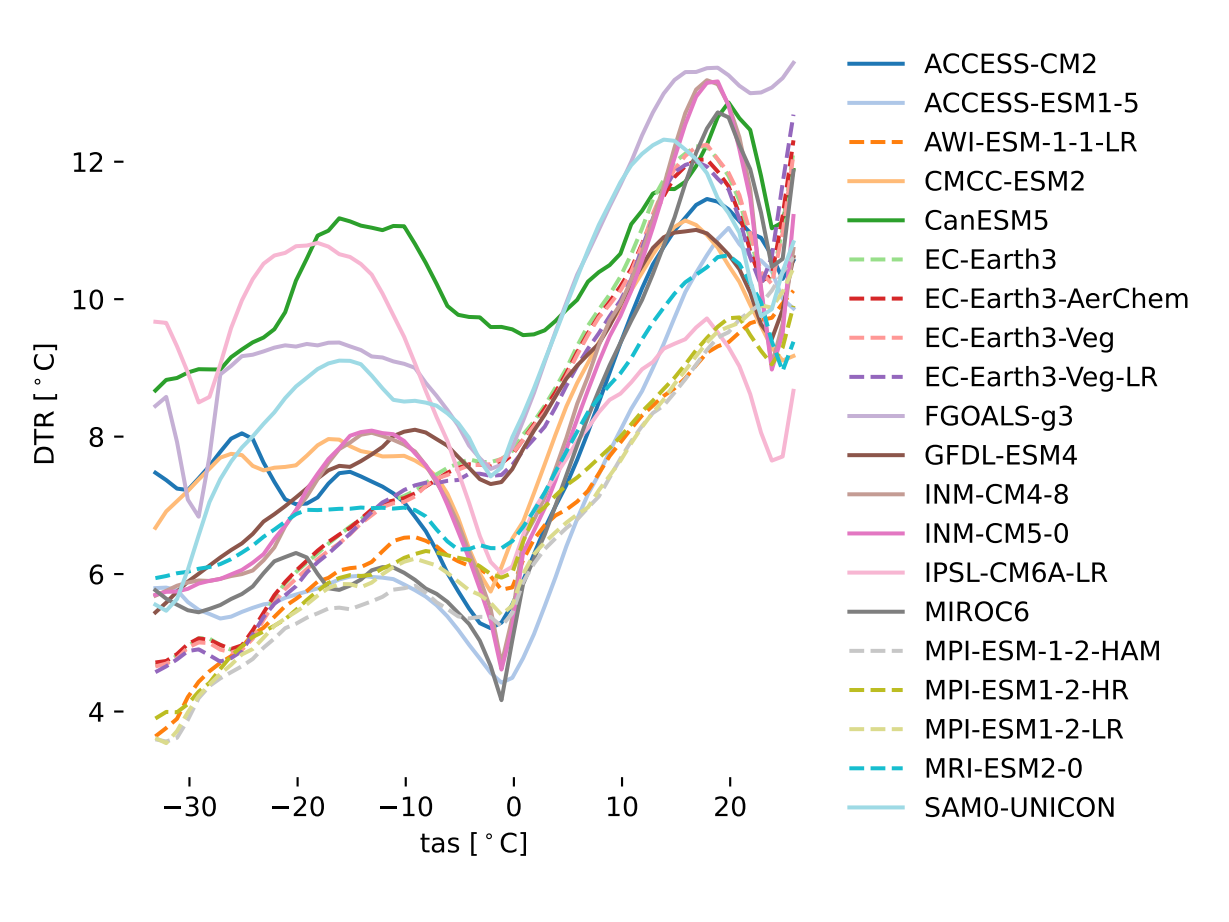
DTR [° C]
12
10
8
6
4
−30
−20
−10
0
10
20
tas [° C]
ACCESS-CM2
ACCESS-ESM1-5
AWI-ESM-1-1-LR
CMCC-ESM2
CanESM5
EC-Earth3
EC-Earth3-AerChem
EC-Earth3-Veg
EC-Earth3-Veg-LR
FGOALS-g3
GFDL-ESM4
INM-CM4-8
INM-CM5-0
IPSL-CM6A-LR
MIROC6
MPI-ESM-1-2-HAM
MPI-ESM1-2-HR
MPI-ESM1-2-LR
MRI-ESM2-0
SAM0-UNICON

Figure 2.

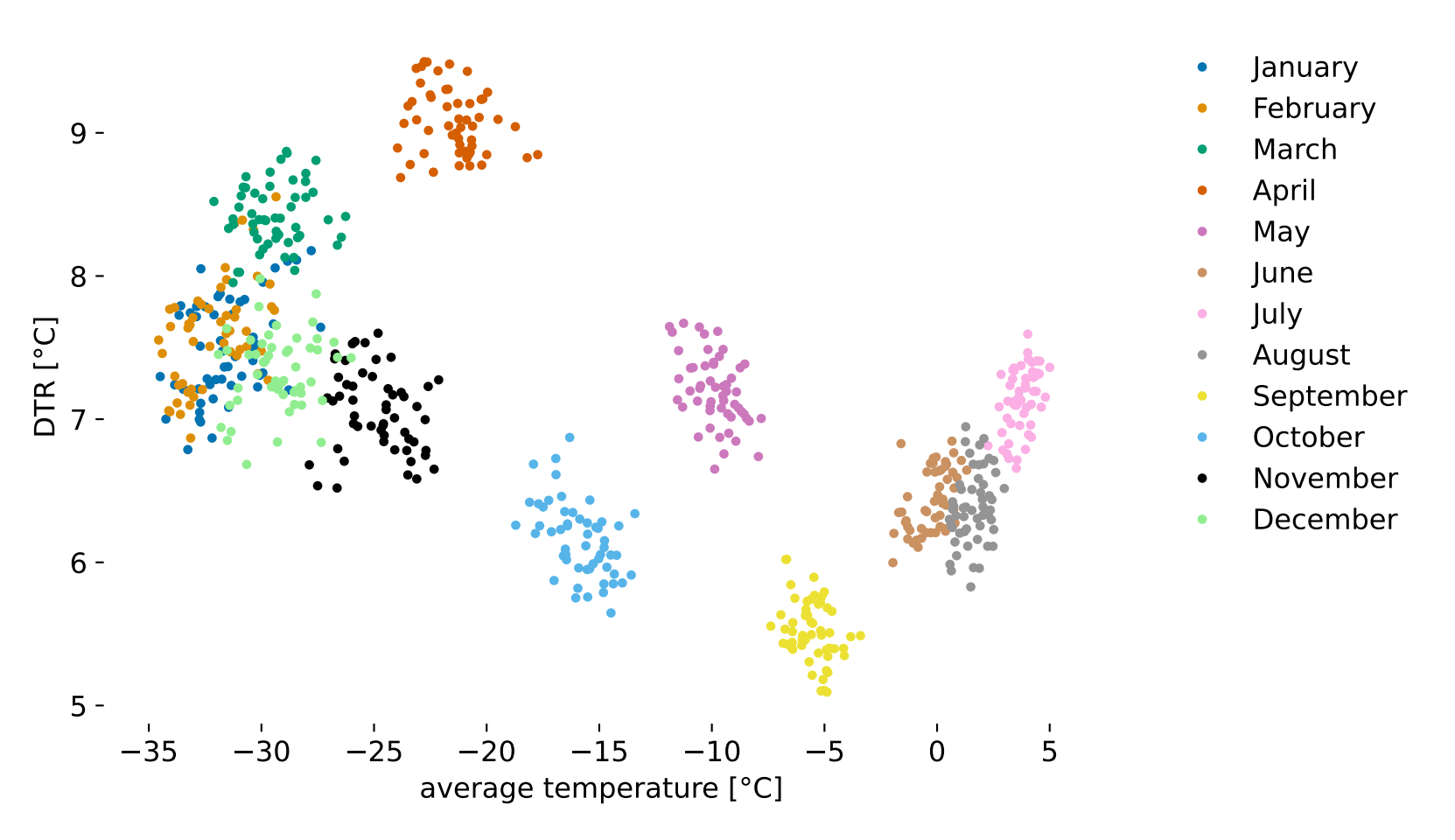
DTR [°C]
9
8
7
6
5
−35
−30
−25
−20
−15
−10
−5
0
5
average temperature [°C]
January
February
March
April
May
June
July
August
September
October
November
December

Figure 1.

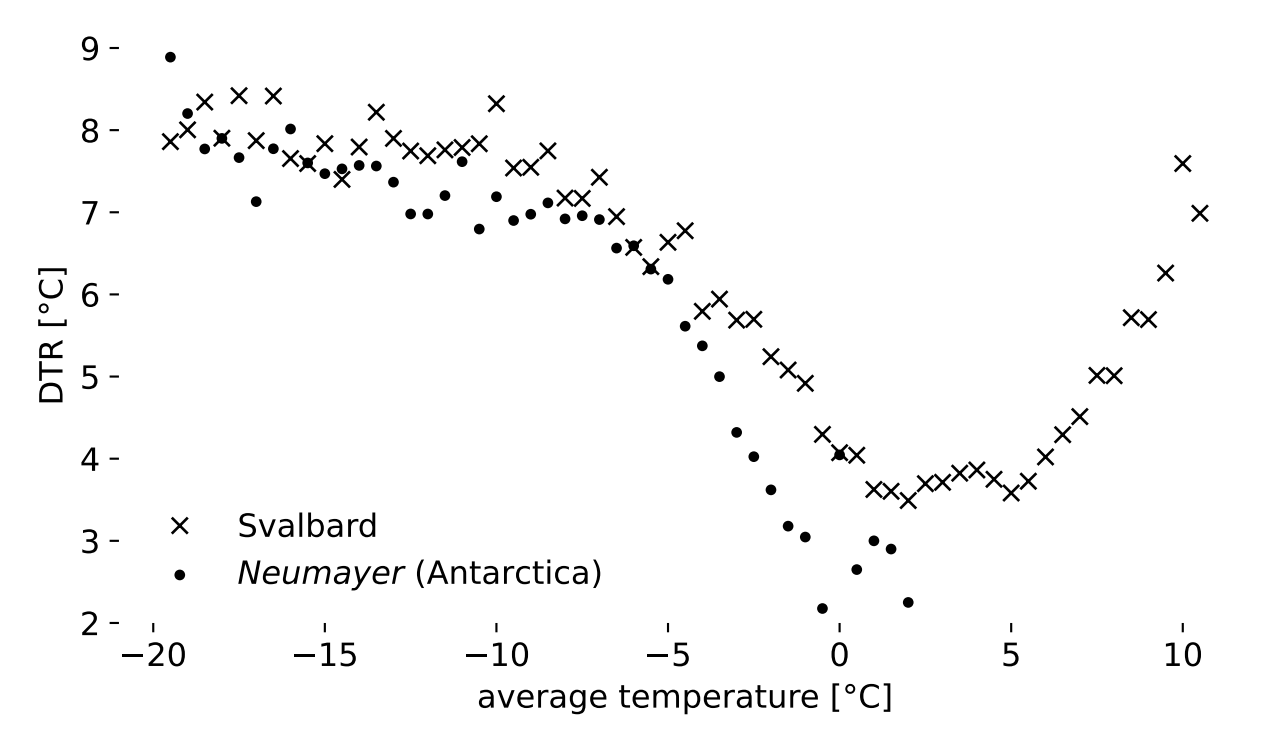
9
8
7
6
5
4
3
2
DTR [°C]
−20
−15
−10
−5
0
5
10
average temperature [°C]
Svalbard
Neumayer (Antarctica)